ELSEVIER

Journal of Fluids and Structures 23 (2007) 569–587

JOURNAL OF FLUIDS AND STRUCTURES

www.elsevier.com/locate/jfs

Dynamics of cantilevered pipes conveying fluid. Part 2: Dynamics of the system with intermediate spring support

M.P. Païdoussis*, C. Semler, M. Wadham-Gagnon, S. Saaid

Department of Mechanical Engineering, McGill University, 817 Sherbrooke St. West, Montréal, Québec, Canada H3A 2K6

Received 20 December 2005; accepted 20 October 2006
Available online 26 December 2006

Abstract

This paper, the second in a three-part series, deals with the three-dimensional (3-D) nonlinear dynamics of a vertical cantilevered pipe conveying fluid, additionally constrained by arrays of four or two springs or a single spring at a point along its length. Theoretical calculations are presented for the same pipe but different spring configurations, points of attachment and stiffnesses, the main generic difference being this: in some cases, the system loses stability by planar flutter, and thereafter performs two-dimensional (2-D) or 3-D periodic, quasiperiodic and chaotic oscillations; in other cases, the system loses stability by divergence, followed at higher flows by oscillations in the plane of divergence or perpendicular to it, again periodic, quasiperiodic or chaotic. Experiments were conducted for some of the systems studied theoretically, and agreement is found to be generally good, although some open questions remain.

Keywords: Pipe conveying fluid; Cantilevered; Nonlinear dynamics; Additional intermediate spring support; 2-D; 3-D motions; Divergence; Flutter; Theory; Experiments

1. Introduction

The problem of a cantilevered pipe with added supports (somewhere along the length, between the fixed and the free end) or added springs has been studied extensively in the past, for it results in much more complex and interesting dynamics, as reviewed in Païdoussis (1998, Sections 3.6 and 5.8) both in the linear and nonlinear domains. All these studies were motivated by the following. On the one hand, a pipe with supported ends is an inherently conservative system (i.e., conservative in the absence of dissipation) and loses stability by divergence via a pitchfork bifurcation; on the other hand, a cantilevered pipe is an inherently nonconservative system, and it loses stability by flutter via a Hopf bifurcation. The question is: what is the dynamical behaviour if an "intermediate" support is provided to a cantilevered pipe, i.e., a support not at the free end? Does the system behave like one with supported ends, or basically as a cantilever?

Some linear studies with a simple support between the fixed (at $x = 0$) and free ($x = L$) ends were first undertaken by Chen and Jendrzejczyk (1985), Edelstein and Chen (1985) and Jendrzejczyk and Chen (1985), showing that, if the support is sufficiently upstream, the pipe behaves as a cantilever, whereas if sufficiently downstream, it behaves as a

*Corresponding author. Tel.: +1 514 398 6294; fax: +1 514 398 7365.
E-mail address: mary.fiorilli@mcgill.ca (M.P. Païdoussis).

0889-9746/$ - see front matter © 2006 Elsevier Ltd. All rights reserved.
doi:10.1016/j.jfluidstructs.2006.10.009

system with supported ends, losing stability by flutter and divergence, respectively. Experiments were also conducted, and the agreement achieved with the linear theory is excellent.

Linear work involving a *flexible* support (a spring), again somewhere between $x = 0$ and L, was also undertaken, notably by Chen (1971a,b) and Sugiyama et al. (1985); the latter also conducted experiments—again achieving quite good agreement with the linear theory. For a fixed position of the spring, say at $x = \frac{1}{2}L$, for a sufficiently weak spring constant, the system behaved as a cantilever, losing stability by flutter; a sufficiently stiff spring, however, made the system lose stability by divergence, as if it were a pipe with supported extremities.

Additional work involving, for example, several spring supports, or a rotational spring in addition to or instead of the translational spring support, are also reviewed in Païdoussis (1998, Section 3.6).

All of the foregoing involved planar (2-D) motions and, in the theoretical work, linear modelling.

Fundamentally, to get a "feel" of the basic dynamics, one can conduct a simple experiment involving a hanging cantilevered pipe conveying fluid—say, air or water. At a flow velocity slightly below what would initiate flutter, merely touching the edge of the pipe with a finger, near the free end, will cause the pipe to buckle. If the finger touches the pipe closer to the clamped end, the pipe does not buckle, but it will eventually begin to flutter as the flow velocity is increased further. Similarly, when an array of intermediate springs is connected to a cantilevered pipe conveying fluid, depending on the individual stiffness k of the springs and the position L_s along the pipe, the pipe will lose stability by either divergence or flutter: the simply supported case corresponds to a spring of infinite stiffness at $L_s = L$, while $k = 0$ is equivalent to a free end. However, as the flow velocity is increased further, the pipe may then develop other instabilities as well; e.g., flutter, if initial loss of stability was by divergence. As the flow rate is increased even further, the pipe may experience three-dimensional (3-D) motion, which does not occur for a plain (i.e., with no intermediate spring supports) cantilevered or simply supported pipe, as will be discussed later in this paper. Thus, it is obvious that 3-D nonlinear theory is required, if the behaviour past the first instability is to be predicted reliably.

Nonlinear theory is also necessary in studying the dynamics in the neighbourhood of double degeneracy, i.e., for the case where the intermediate support is such that the two bifurcations (pitchfork and Hopf) occur simultaneously at a critical flow velocity. It is known that in the neighbourhood of double degeneracy, interesting dynamical behaviour may

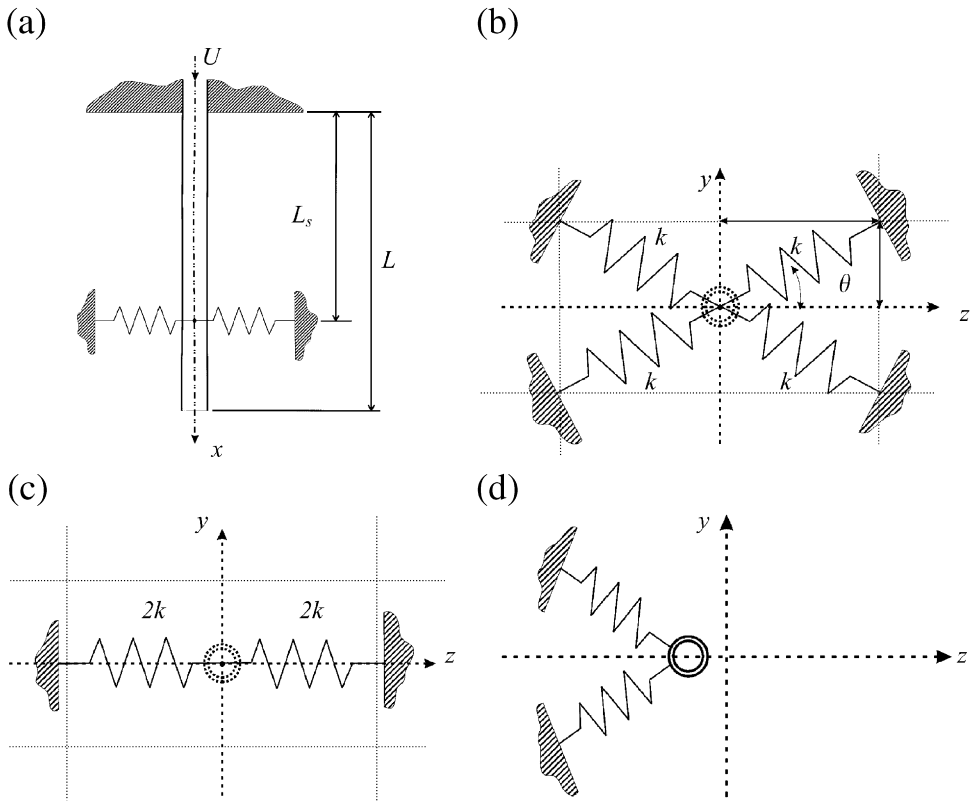

Fig. 1. (a) Schematic representation of side view of the system, (b) the four-spring configuration, located along the pipe at $x = L_s$, (c) the special case of the four-spring array in (b) with $\theta = 0$, (d) the pre-stressed two-spring arrangement.

arise, including the possibility of chaos, basically because the system "cannot decide" whether it should diverge statically or flutter, or do both at once; i.e., the system might "hunt" aperiodically between two attractors.

One such theoretical study was undertaken by Païdoussis and Semler (1993), involving a linear spring (geometrically linear also, by presuming the spring to be attached to a sliding support). In this work, motions were considered to be two-dimensional (2-D), i.e., planar. Some interesting analytical work was conducted, involving normal forms and centre manifold theory, and heteroclinic orbits were found to arise for some sets of system parameters. It is known that if such orbits are perturbed, heteroclinic tangles and chaos may be generated (Guckenheimer and Holmes, 1983; Moon, 1992). Indeed, chaos was found to occur if the system was given periodic perturbation in the flow velocity.

The more general case of 3-D motions of a pipe with intermediate spring supports was tackled by Steindl and Troger (1996), who considered in depth the regions of existence and stability of heteroclinic cycles, again in the neighbourhood of double degeneracy, involving pitchfork and Hopf bifurcations of the system. Also, Steindl (1996) considered another type of heteroclinic cycle, associated with Hopf–Hopf bifurcations.

Apart from earlier linear work, there is paucity of experimental investigations into such systems in the nonlinear realm, which would permit the study of the dynamics beyond the first loss of stability. One such study was made by Saaid (1999) who investigated the problem both theoretically and experimentally. The experiments will be discussed in this paper. The theory used by Saaid was an earlier, 2-D version of that of Part 1 (Wadham-Gagnon et al., 2007) of this study, in which the induced tension due to vertical lifting of the point of attachment of the springs on the pipe (significant at large pipe deflections) is not taken into account. Hence, Saaid's experiments are compared in this paper with the improved theory in which the vertical lifting of the pipe is accounted for.

The system under consideration is shown schematically in Fig. 1(a). Fig. 1(b)–(d), shows the different spring arrangements (all at $x = L_s$) investigated, both theoretically and experimentally, as will be discussed in what follows.

2. Theoretical dynamics

Using the inextensibility conditions, the 3-D dynamics is described by two nonlinear coupled partial differential equations, as derived in Part 1 (Wadham-Gagnon et al., 2007). These equations are then transformed into a set of eight nonlinear second-order ordinary differential equations using a Galerkin approach with four beam-mode comparison functions in each orthogonal direction, y and z (or $\eta = y/L$ and $\zeta = z/L$ in dimensionless form). A finite difference scheme is then applied to the Galerkin-type solution, yielding the displacements $\eta(\xi, \tau)$ and $\zeta(\xi,\tau)$, where $\xi = x/L$ and τ is dimensionless time.

In this section, a theoretical study is presented through a series of simulations for the system with parameters given in Table 1, which corresponds to the pipe used in the experimental study discussed in Sections 3 and 4. The dimensionless parameters, as defined in Eq. (42) of Part 1, become $\beta = M/(M+m) = 0.145$ and $\gamma = (M+m)gL^3/EI = 25.4$, where the symbols are defined in Table 1.

The physical parameters that can easily be varied are: (i) the flow velocity, U, and its dimensionless counterpart, u, (ii) the individual spring stiffness, k, (iii) the initial stretch in each spring with respect to the centreline of the pipe at rest, $(R_o–L_o)$, (iv) the absolute angle of an individual spring with respect to the z-axis, θ, (v) the point of attachment of the array of springs along the pipe, L_s, (vi) the number of springs in the array, either 2 or 4 corresponding to the configurations of Figs. 3 and 4 of Part 1 and Fig. 1 here.

In order to describe a wide spectrum of results, five qualitatively different cases are explored numerically in this work, as defined in Table 2. It was originally supposed that the most interesting dynamics would arise in the close vicinity of the pitchfork/Hopf bifurcation double degeneracy. This would occur if the location and stiffness of the springs were such that the pitchfork bifurcation (leading to static divergence) and the Hopf bifurcation (leading to flutter) occurred simultaneously, at the same flow velocity, as predicted by linear theory. Experiments showed that the situation of the

Table 1
Pipe parameters used in the calculations

Length, L	0.443 m
Inner/outer diameter, D_i/D_o	6.4/15.7 mm
Flexural rigidity, EI	7.42×10^{-3} N m^2
Density of the pipe, ρ_p	1167 kg/m^3
Density of the fluid, ρ_f	999 kg/m^3
Mass per unit length of pipe, m	0.189 kg/m
Mass per unit length of fluid, M	0.0320 kg/m

Table 2
Spring parameters for the different theoretical cases studied

	Case 1	Case 2	Case 3	Case 4	Case 5
Springs	4	4	4	2	2
L_s	$0.6L$	$0.75L$	$0.75L$	$0.75L$	$0.75L$
θ	12.80°	27.11°	0°	10°	0°
k (N/m)	17.63	17.63	17.63	22	20
R_o (m)	0.1062	0.0727	0.0727	0.0727	0.0727
L_o (m)	0.0635	0.0635	0.0635	0.0635	0.0635

system "hunting" between these two different behavioural patterns never arises. Nevertheless, the most interesting dynamics was observed in the wider neighbourhood of this double degeneracy. It was on these spring locations that the experimental programme focussed, and hence also the theoretical calculations.

Theoretical calculations for each of the five cases in Table 2 will now be presented in the following subsections.

2.1. Initial instability via Hopf bifurcation (dynamic instability)—Case 1 in Table 2

The first spring configuration studied is chosen such that the system first loses stability via a Hopf bifurcation (i.e., similarly to the plain cantilevered pipe). The four-spring array is fixed at $L_s = 0.6L$ and the angle at equilibrium of each spring with respect to the z-axis (ζ-axis) is $\theta = 12.80°$. The overall dynamics of the system is summarized in the bifurcation diagram of Fig. 2, where the orthogonal displacements, η and ζ, at the tip of the pipe are plotted when their respective velocities, $\dot{\eta}$ and $\dot{\zeta}$ change sign, i.e., reach a local minimum/maximum, as a function of flow rate. As expected, the system is stable for small flow velocities; it then loses stability at dimensionless flow velocity $u_{cr} = 8.8$, where planar flutter starts to occur in the xy-plane. An inspection of the linear coefficients of the spring forces acting on the system [Eqs. (28) and (29) of Part 1] shows that these periodic oscillations occur in the plane of *least* resistance, i.e., in the xy-plane here. For the system concerned, typical planar flutter, very similar to that occurring for a plain cantilevered pipe, for a flow velocity of $u = 10.0$ is shown in the time trace of Fig. 3(a), the phase plane diagram of Fig. 3(b) and the pipe shape over a cycle of oscillation of frequency $f = 7.0$[1] in Fig. 3(c). Although comparable to the flutter of a plain pipe, the instability here occurs at a much higher flow rate with a much higher frequency [Païdoussis and Semler (1993) found $u_{cr} \approx 5.5$ and $f \approx 2.5$ for a similar plain pipe].

A pitchfork, or symmetry breaking bifurcation, occurs at $u = 12.2$: the pipe oscillates asymmetrically, giving preference to one side of the original equilibrium configuration, as determined by the initial conditions (only one such solution is shown in the bifurcation diagram of Fig. 2 for simplicity). Symmetry is regained afterwards at $u = 13.4$, and retained until $u = 14.8$. There is no unusual change in frequency before, throughout and after the symmetry break, apart from the continuous increase in frequency due to the increasing flow rate. At a flow velocity of $u = 15$, quasiperiodic oscillations take place, followed almost immediately by a new qualitative solution: periodic oscillations having a much larger frequency and smaller amplitudes (at $u = 15.2$).

Up to this point, all the dynamics occur in one plane and it is very similar to what was described by Païdoussis and Semler (1993), except for the jump in frequency at $u = 15.2$. No such jump was reported by Païdoussis and Semler (1993); but, in that study, only two Galerkin modes were used for discretizing the system.[2]

As shown in Figs. 2 and 4, the first sign of 3-D motion ensues at a flow rate of $u = 15.4$ (note the appearance of crosses in the bifurcation diagram). It is characterized by quasiperiodic deviations from the initial plane of oscillation. A fast Fourier transform applied to the time trace of Fig. 4(a) shows a dominant frequency of $f = 12.1$, but it takes approximately three of these partial cycles for the pipe to complete a quasiperiodic cycle, such as shown in Fig. 4(b). The projection onto the zx-plane of the pipe shape in Fig. 4(e) over a partial cycle shows that the response in that plane is not symmetrical, while it is so in the xy-plane [Fig. 4(d)]. Note how the pipe shape is clearly influenced by the position of the springs, $L_s = 0.6L$, this node being nearly stationary. Fig. 4(d), when compared to Fig. 3(c), shows the radical change in pipe shape over a cycle of oscillation due to the bifurcation associated with 3-D motion and a jump in frequency.

[1]The frequencies quoted are in dimensionless Hz, rather than dimensionless rad/s.

[2]It may be of interest that a similar frequency jump has been reported for the system with an end-mass (Païdoussis and Semler, 1998).

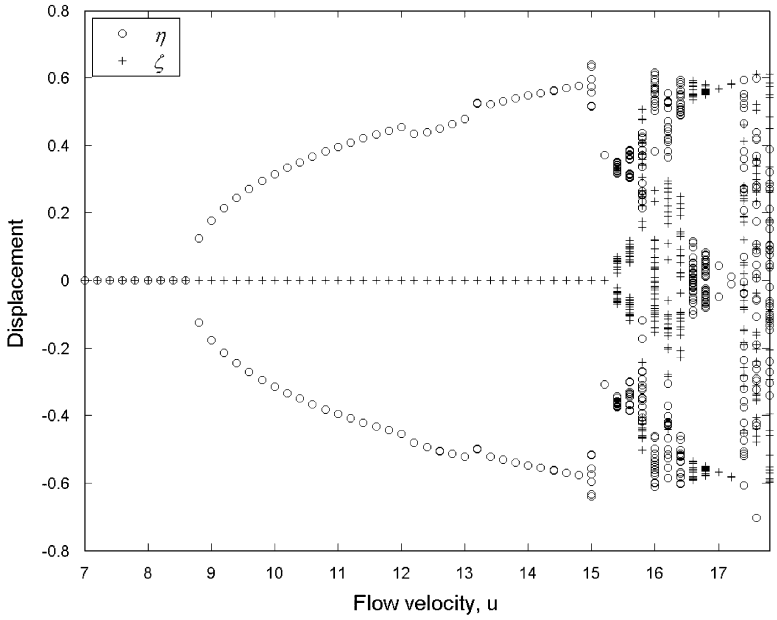

Fig. 2. Bifurcation diagram for Case 1: four-spring array, $L_s = 0.6L$, $\theta = 12.80^\circ$, $k = 17.63\,\mathrm{N/m}$, $R_o = 0.1062\,\mathrm{m}$ $(R_o–L_o) = 0.0427\,\mathrm{m}$. Note that circles (o) denote dimensionless displacements η in the xy-plane (see Fig. 1), while crosses (+) refer to displacements ζ in the zx-plane.

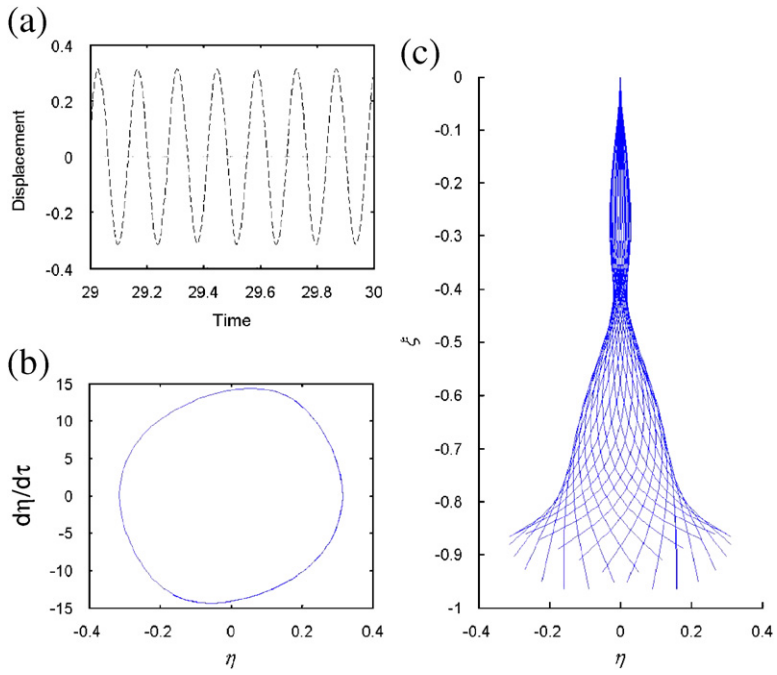

Fig. 3. Case 1 at $u = 10.0$: (a) time trace of tip displacement (– –, η; —, ζ). (b) Phase plane diagram of tip displacement ($\zeta = 0$) for $29 \leqslant \tau \leqslant 30$. (c) Pipe shape in the xy-plane over a period of frequency $f = 7.0$ starting at time $\tau = 29$.

A few quasiperiodic cycles later, the mirror image of Figs. 4(b) and (d) is obtained, which clarifies the symmetry of the surface covered by the projection of the tip displacement on to the yz-plane over a longer period of time provided in Fig. 4(c). The overall symmetry over time indicates that the dynamics is not a result of a pitchfork bifurcation, while the

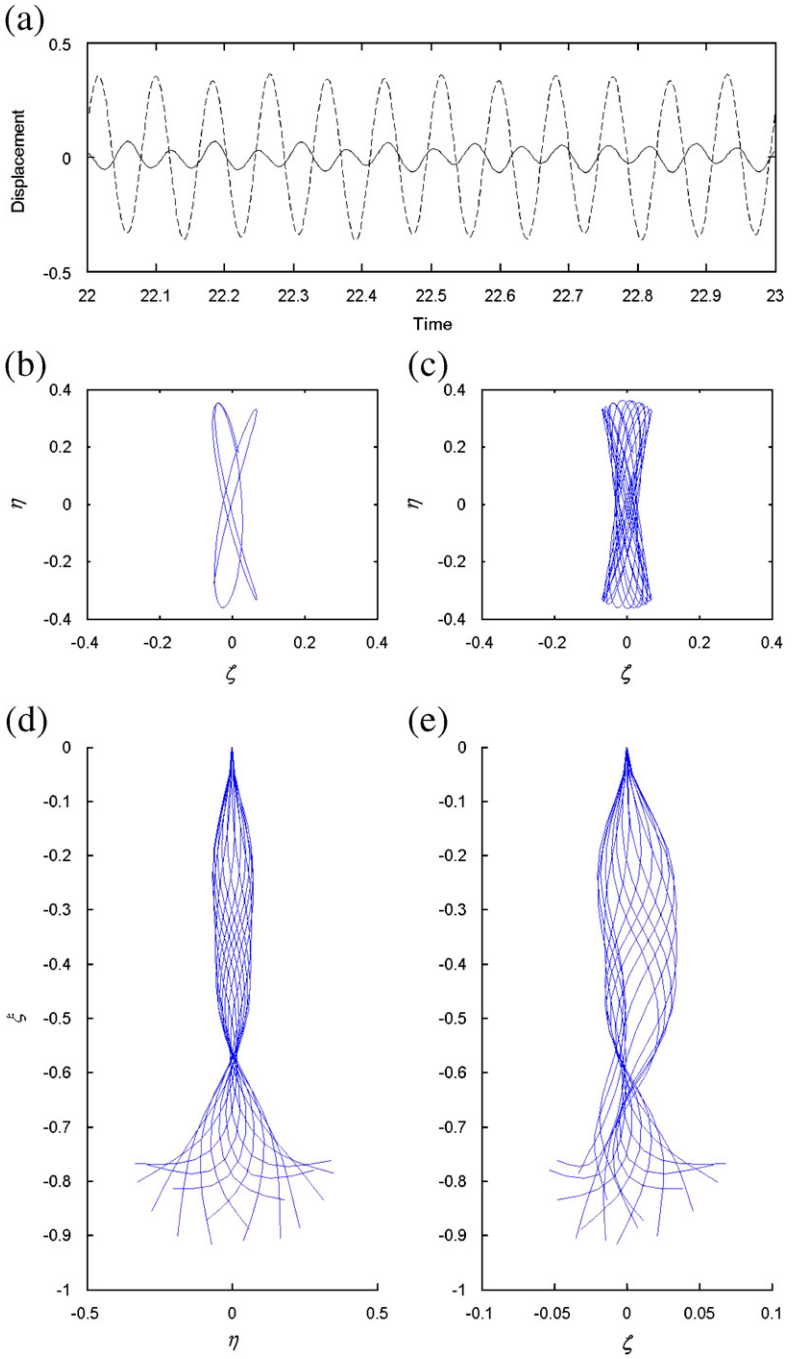

Fig. 4. Case 1 at $u = 15.4$: (a) time trace of tip displacement (– –, η; —, ζ). (b,c) Tip displacement projected onto the yz-plane, in (b) over a cycle of dimensionless frequency $f = 4.7$, and in (c) over several cycles. (d,e) Pipe shape over a period of frequency $f = 12.1$ starting at time $\tau = 22$, projected onto, (d) the xy-plane, and (e) the zx-plane (note the difference in the scale of the abscissa).

seemingly asymmetrical behaviour is purely a 3-D quasiperiodic effect of the system. It should be noted that although 3-D, the motion in the zx-plane remains small *vis-à-vis* that in the xy-plane.

As the flow rate is increased further, chaotic oscillations take place between $u = 15.8$ and 16.4. The system briefly returns to quasiperiodic behaviour between $u = 16.6$ and 16.8 and even periodic behaviour between $u = 17.0$ and 17.2. The time trace of the tip displacement given in Fig. 5(a) and the projection of the tip displacement in the yz-plane of

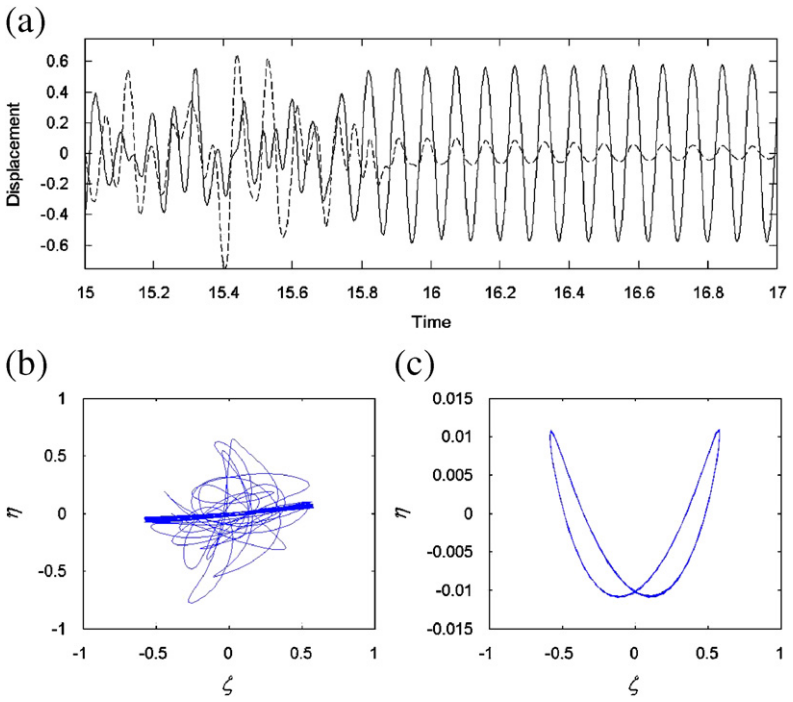

Fig. 5. Case 1 at $u = 17.2$: (a) time trace of tip displacement (– –, η; —, ζ). (b,c) Tip displacement projected onto the yz-plane for (b) $\tau = 15$–20 and (c) $\tau = 24.5$–25.

Fig. 5(b), for $u = 17.2$, shows that the pipe undergoes transient chaotic oscillations for the first 16 dimensionless time units before "stabilizing". Even so, it is not until $\tau \approx 20.0$ that the periodic limit cycle is fully established. This simply points out how the system "may take time" to settle down into a quasiperiodic or even periodic state. A transition phase before reaching the state of steady oscillation happens in all simulations (if there exists a steady solution); it is only a matter of how long it takes before it is reached. For a plain pipe near the point of Hopf bifurcation, due to the small effective damping of the system, steady state is reached after a long period of time and with decaying or climbing amplitude, depending on initial conditions. Here, the steady state is not even perceptible until it suddenly falls into place around $\tau \approx 16$. It is noted that the plane of symmetry has been interchanged with respect to the results in Fig. 4.

The dynamics of this system at higher flow velocities ($u > 17.2$) is assumed to be chaotic (for simulations tested up to $\tau \approx 100$).

2.2. Initial instability via pitchfork bifurcation (static instability)—Case 2 in Table 2

In this second case, the array of four springs is positioned closer to the free-end (at $L_s = 0.75L$) and the total stiffness of the springs is large enough for the pipe to initially lose stability via a pitchfork bifurcation. Here, the spring angle with respect to the z-axis is $\theta = 27.11^\circ$ and the initial stretch in each spring is $(R_o – L_o) = 0.0092$ m. As seen in the bifurcation diagram of Fig. 6, divergence occurs at a flow rate of $u = 7.3$. Referring again to the spring forces acting on the pipe, given in Eqs. (28) and (29) of Part 1, the buckling here occurs in the plane of *most* resistance, i.e., the zx-plane which is opposite to the case where stability is lost by a Hopf bifurcation described in Section 2.1, which seems sound from a theoretical point of view. This will be discussed in-depth in Section 4, following the experimental results.

The "asymmetrical" shape of the buckled pipe, represented by a nonzero fixed point in the bifurcation theory nomenclature, has a symmetrical counterpart which can be obtained by using opposite-sign initial conditions, not shown, again for clarity. As can be seen in Fig. 6 for $7.3 < u < 8.3$, the amplitude of divergence increases with the flow rate.

At $u = 8.3$, the nonzero static and planar solution becomes unstable through a Hopf bifurcation. This not only results in oscillations around the unstable fixed point, but also in periodic and symmetric oscillations in the perpendicular plane. This 3-D periodic behaviour soon becomes quasiperiodic at $u = 8.6$. An example of quasiperiodic oscillations is given in Fig. 7 for a flow rate of $u = 10.0$. The time trace of the tip of the pipe in Fig. 7(a) shows a

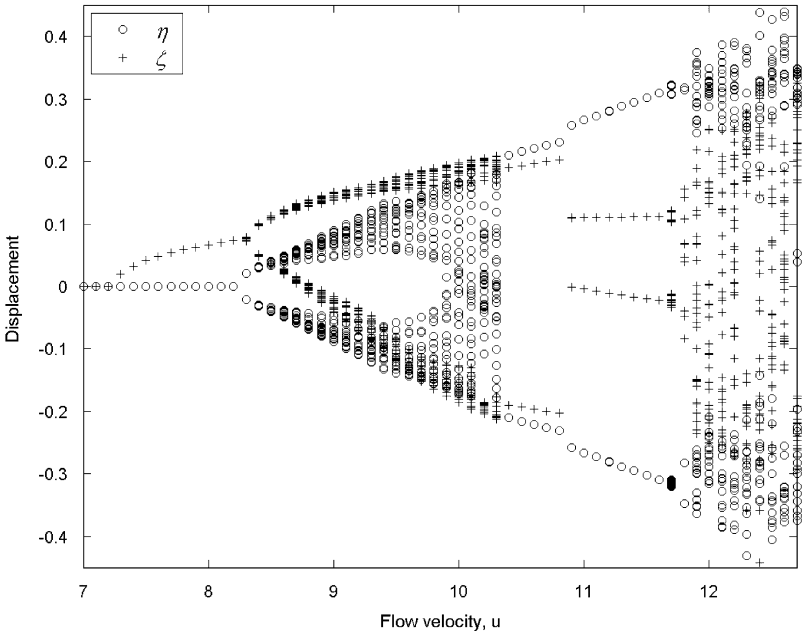

Fig. 6. Bifurcation diagram for Case 2; four-spring array, $L_s = 0.75L$, $\theta = 27.11^\circ$, $k = 17.63\,\mathrm{N/m}$, $R_o = 0.0727\,\mathrm{m}$ $(R_o–L_o) = 0.0092\,\mathrm{m}$.

dominant frequency, $f = 9.0$, but also a recurring cycle with a period of $\tau \approx 3.75$. Although Fig. 7(b) shows no sign of symmetry over a short time interval of frequency $f = 9.0$, Fig. 7(c) suggests there is an overall symmetry over a longer time interval. It is seen in Figs. 7(d) and (e) that in the xy-plane the system performs small oscillations superposed on the state of divergence. Moreover, the system undergoes a "dynamic" divergence behaviour, in that the side to which the buckling occurs switches aperiodically, as illustrated for $\tau = 12$ and 14 in Figs. 7(d) and (e).

A return to periodicity beginning at $u = 10.4$ follows, where the tip displacement traces an oval shape in the yz-plane, as shown in Fig. 8(a) for a flow velocity of $u = 10.6$. This figure also suggests that the system has found another plane of symmetry, other than the xy- or zx-plane. At a flow rate of $u = 10.9$, the trace of the tip displacement becomes a figure-of-eight as shown in Fig. 8(b) for $u = 11.0$, and the transition from the oval shape to the figure-of-eight shape periodic oscillations seems to occur with no sign of a transitional quasiperiodic or chaotic phase. The figure-of-eight phase is once again characterised by a dynamic behaviour about a point of divergence in the zx-plane while oscillating symmetrically in the xy-plane.

There is a short transition from periodic to quasiperiodic motion between $u = 11.7$ and 11.9; the system then becomes chaotic, as shown in Fig. 9 for a flow rate of $u = 12.5$, before the numerical solution "crashes" due to matrix singularities.

2.3. *Special case of the four-spring array: $\theta = 0^\circ$—Case 3 in Table 2*

Using the same parameters as in Case 2 while changing only the absolute spring angle with respect to the z-axis to $\theta = 0^\circ$ leads to an equivalent system with only two springs on either side of the pipe, along the z-axis—see Fig. 1(c).

The bifurcation diagram in Fig. 10 shows that the system loses stability via a pitchfork bifurcation at a flow rate of $u = 7.2$, in the plane of the springs (the zx-plane). The solution remains static until $u = 8.3$, where it becomes dynamic through a Hopf bifurcation, with oscillations emerging about the now unstable point of divergence. The response is still in the plane of initial buckling and is referred to as "in-plane flutter". Eventually, at $u = 8.8$, the pipe loses stability in the perpendicular plane (xy-plane) as well, leading to 3-D quasiperiodic (figure-of-eight shape) oscillations.

As the flow rate is increased, an interesting quasiperiodic solution occurs, shown in Fig. 11 for $u = 9.0$. The system leaves the impression of cyclically fluctuating from "in-plane flutter" to "figure-of-eight" oscillations. Indeed, as seen in the time trace of Fig. 11(a) the oscillations in the xy-plane undergo large variations in amplitude. The system is nonetheless globally stable and completes a full, quasiperiodic, cycle in $\tau \approx 5$, typically projecting the tip displacement over one cycle into the yz-plane, as shown in Fig. 11(b). A fast Fourier transform reveals that the oscillations in the

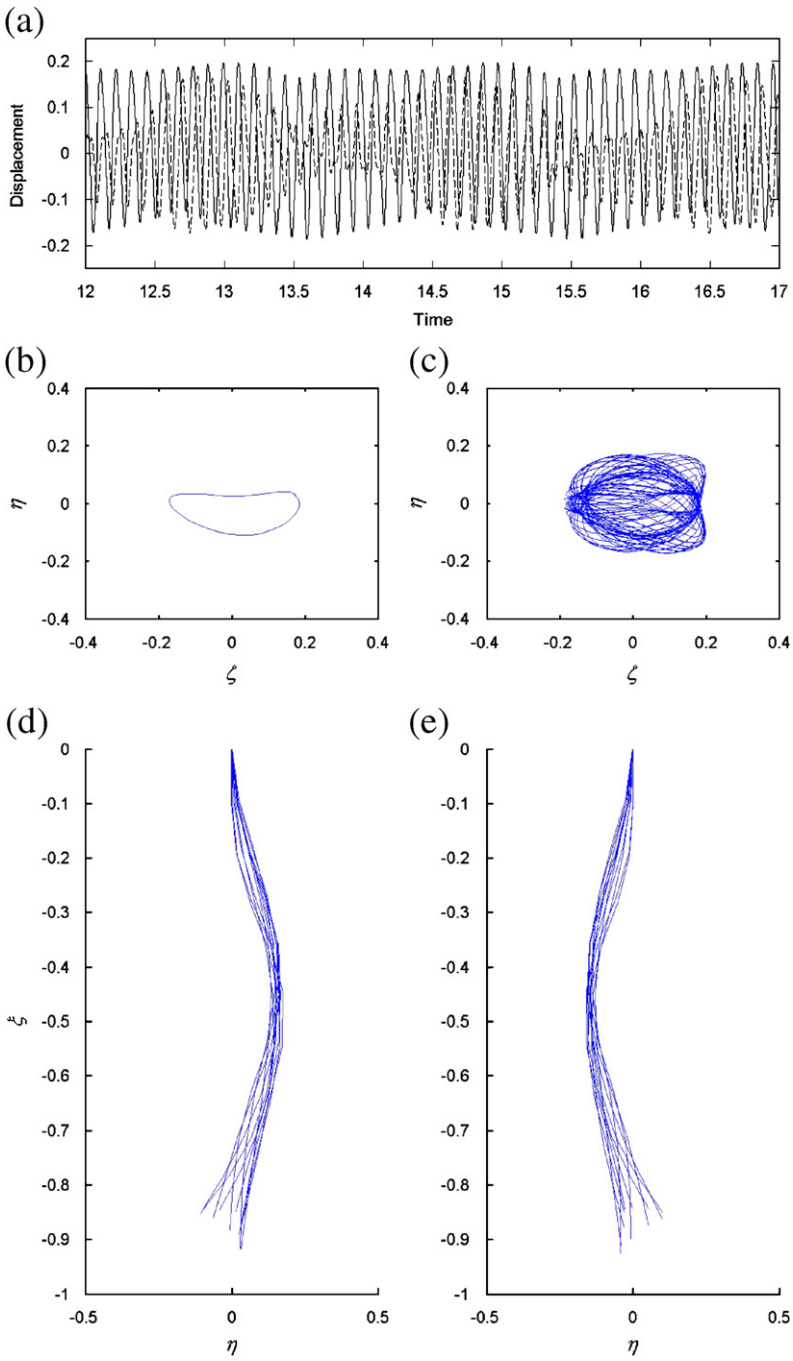

Fig. 7. Case 2, quasiperiodic oscillations at $u = 10.0$: (a) time trace of tip displacement (– –, η; —, ζ). (b,c) Tip displacement projected onto the yz-plane; (b) over a quasi-cycle of oscillation of frequency $f = 9.0$, and (c) for $\tau = 12$–17. (d,e) Pipe shape over quasi-period of oscillation of frequency $f = 9.0$ projected onto the xy-plane starting at time (d) $\tau = 12$ and (e) $\tau = 14$.

zx-plane have a frequency of $f \approx 9.1$ while the oscillations in the xy-plane have a frequency of $f \approx 4.4$, which is roughly half of that in the zx-plane. In the case of a periodic "figure-of-eight shape" oscillation (e.g., Fig. 8(b)), it is expected that the frequency in one plane is double that in the other plane. Over several cycles, as seen in Fig. 11(c) for $\tau = 0$–100, a clear contour of the projected surface covered by the tip displacement is defined, curiously resembling the shape of a butterfly!

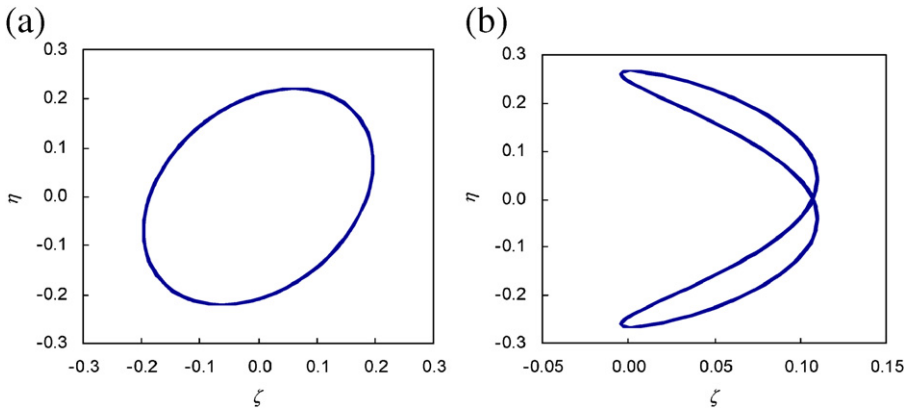

Fig. 8. Periodic tip displacement projections into the *yz*-plane of Case 2 at flow rates (a) $u = 10.6$ and (b) $u = 11.0$.

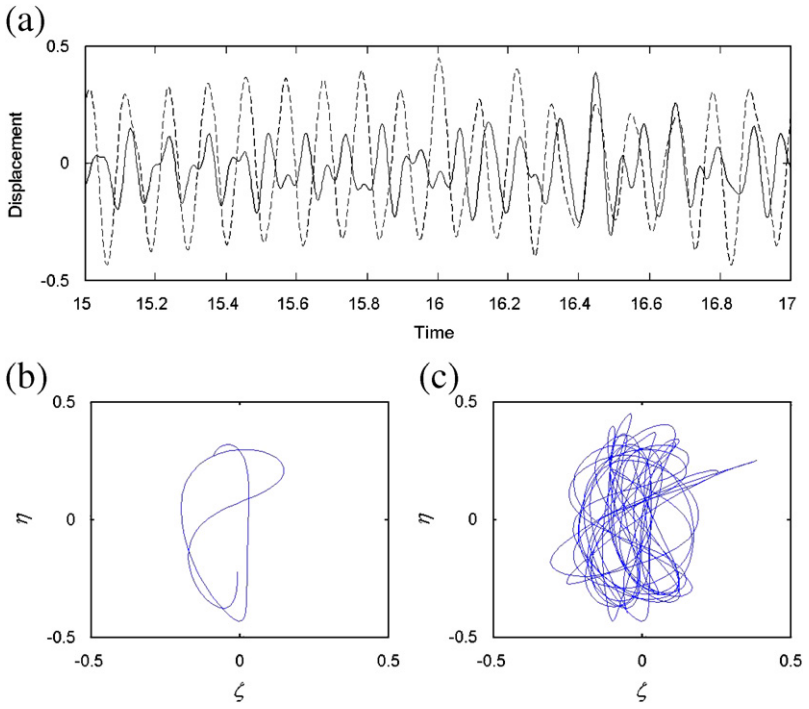

Fig. 9. Case 2 chaotic oscillations at $u = 12.5$: (a) time trace of tip displacement ($- -, \eta$; —, ζ). (b,c) Tip displacement projected onto the *yz*-plane over (b) a short time period and (c) a longer period.

2.4. Two-spring array, general behaviour—Cases 4 and 5 in Table 2

The two-spring array defined in Appendix B of Part 1 is of special interest when $R_0 \neq L_0$, since it introduces an initial constant force on the pipe in the *z*-direction, as seen in Eq. (B.4) of Part 1. The reader is referred to Fig. 4 of Part 1 and Fig. 1(d) here for a schematic representation. Due to the position of the springs, the "unbalanced" force deforms the pipe initially in an almost pure first-mode shape before flow is introduced into the system. This will be referred to as the initial state of the pipe. Two configurations are analysed with the two-spring array: Cases 4 and 5 of Table 2.

For Case 4, it is seen in the bifurcation diagram of Fig. 12(a) that the initial deformation of the pipe is eventually amplified as the flow rate increases, the effects beginning to be noticeable around $u \approx 6.8$. The nonzero static solution

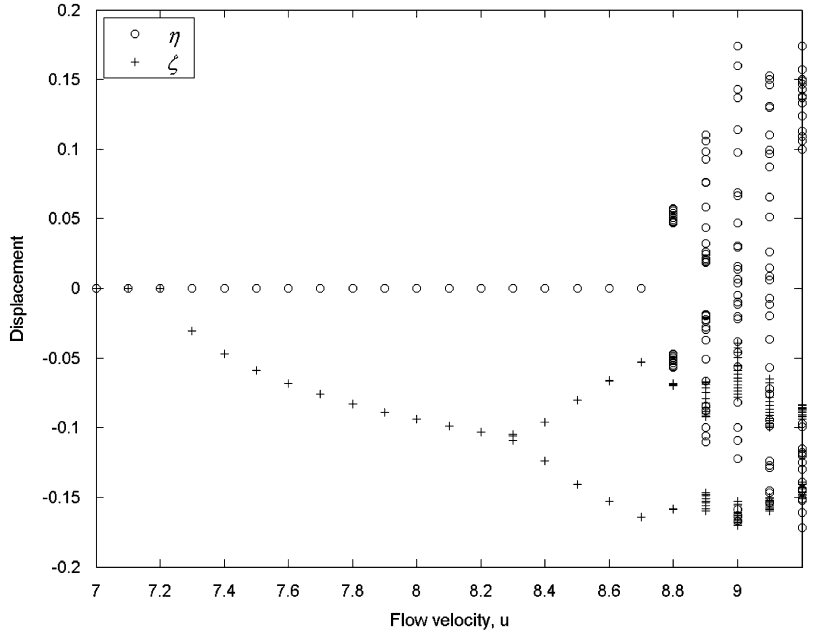

Fig. 10. Bifurcation diagram for Case 3; with the four-spring array, $\theta = 0^\circ$ and $k = 17.63\,\mathrm{N/m}$ (or with the two-spring array, $\theta = 90^\circ$ and $k = 35.26\,\mathrm{N/m}$), $L_s = 0.75L$, $R_o = 0.0727\,\mathrm{m}$ $(R_o–L_o) = 0.0092\,\mathrm{m}$.

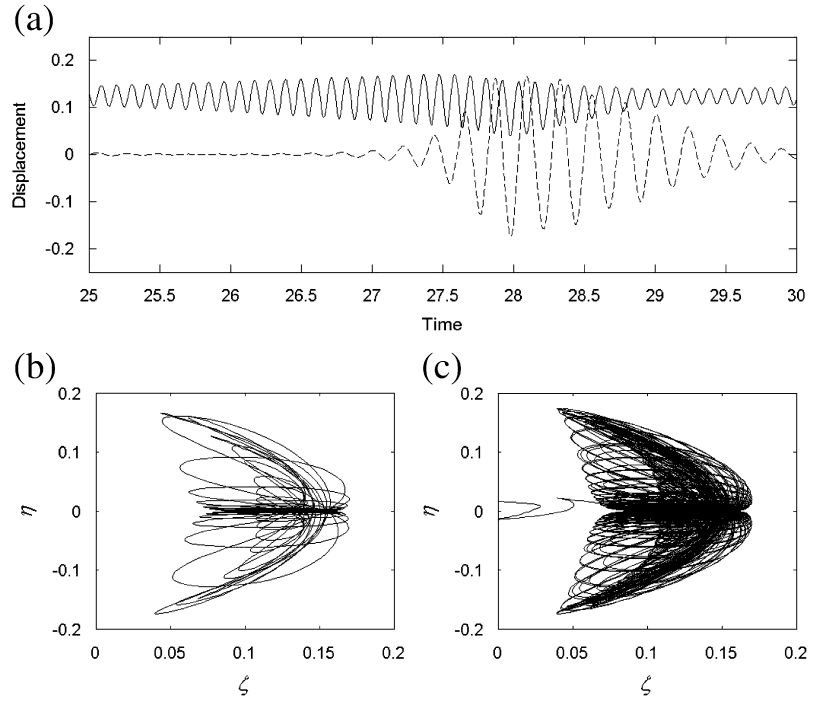

Fig. 11. Case 3, quasiperiodic oscillations at $u = 9.0$: (a) time trace of tip displacement (– –, η; —, ζ). (b,c) Tip displacement projected onto the yz-plane, (b) over a quasi-cycle of transition from in-plane to out-of-plane oscillations of quasi-period $T \approx 5$, and (c) the butterfly: tip displacement over several cycles.

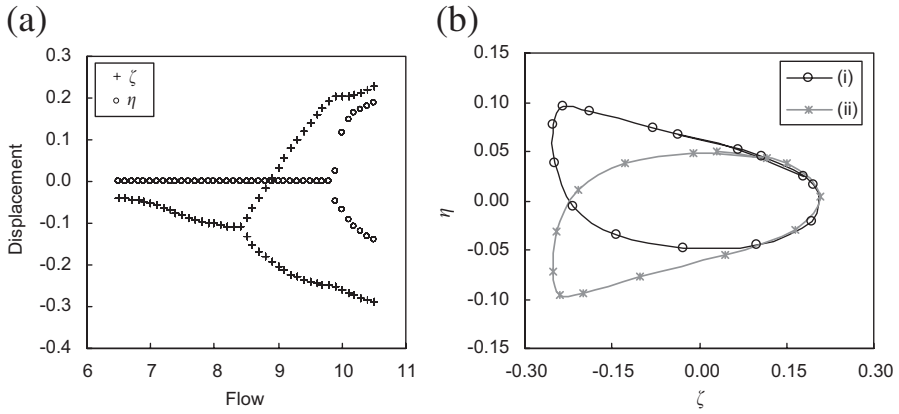

Fig. 12. Case 4: (a) bifurcation diagram, (b) tip displacement limit cycle at $u = 10.0$ for two different sets of initial conditions, (i) and (ii), showing the symmetry with respect to the zx-plane on the y-axis origin.

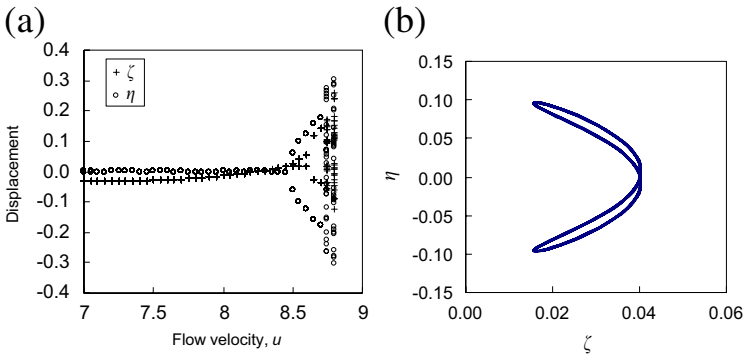

Fig. 13. Case 5; special case of the two-spring array where $\theta = 0^\circ$: (a) bifurcation diagram; (b) tip displacement at $u = 8.55$, showing out-of-plane, "figure-of-eight" flutter.

becomes unstable through a Hopf bifurcation at $u = 8.5$, with in-plane (zx-plane) oscillations developing about the amplified initial state. Then, at $u = 9.9$, 3-D periodic oscillations develop. The motion in the plane perpendicular to the initial state immediately takes an asymmetric form observable through the tip displacement which seems to favour one side of the y-axis or the other, depending on initial conditions, as shown in Fig. 12(b) for a flow velocity $u = 10.0$.

Case 5 is a special case of the two-spring array configuration where the two springs are reduced to a single spring initially along the z-axis, obtained by setting $\theta = 0^\circ$. Again, a pre-tensioned spring causes the pipe to have an initial, nontrivial, state of equilibrium, as seen in the bifurcation diagram of Fig. 13(a). Similarly to the previous case, the fluid being conveyed through the pipe eventually influences its initial state. Contrary to the previous case, the influence of the fluid does not make the tip displacement move in the same direction as in Case 4; rather than moving towards the point of attachment of the springs (and away from the x-axis centreline) the tip displacement in Case 5 moves away from the springs, in the positive z-direction. While the displacement of the tip of the pipe goes in opposite directions, both systems (Cases 4 and 5) globally experience the same phenomenon; amplification of the initial shape of the pipe with increasing flow rate. The difference in the behaviour of the tip displacement can simply be attributed to a combination of different system parameters.

Continuing with the bifurcation diagram for Case 5 (Fig. 13(a)), Hopf bifurcations develop simultaneously at $u = 8.5$ in both planes, leading immediately to 3-D motion, similarly to what is observed in the system of Fig. 6. In this case, the projected tip displacement traces a figure-of-eight limit cycle in the yz-plane, such as shown in Fig. 13(b) for $u = 8.55$. The periodic figure-of-eight motion is characterized by oscillations in the plane of initial divergence with symmetric flutter in the perpendicular plane. The periodic motion persists with increasing amplitude, until chaotic oscillations develop at $u = 8.75$.

3. The experimental investigation

The experimental study was conducted in order to collect some data for a cantilevered pipe conveying fluid with intermediate spring supports, which could be compared with theoretical predictions.

The results collected are in the form of critical flow rates and bifurcation diagrams for Cases 1 and 2. A special experiment was conducted later to verify the effect of the ring attachment connecting the springs to the pipe, which is discussed qualitatively.

3.1. Experimental set-up

The pipe under consideration is specially cast from liquid silicone rubber and catalysed into an elastic solid for which the physical and mechanical properties are listed in Table 1. The modal damping coefficients for the first four modes of the dry pipe (without water in it) were found to be $\delta_1 = 0.036$, $\delta_2 = 0.114$, $\delta_3 = 0.148$, $\delta_4 = 0.293$. Then, by analytically comparing the damping coefficients of both the dry pipe and the wet pipe (accounting for the mass of water in the pipe), one can easily find that the two are related by a factor $(1–\beta)^{1/2}$; thereby, the modal damping coefficients for the wet pipe are $\delta_1^* = 0.033$, $\delta_2^* = 0.105$, $\delta_3^* = 0.137$, $\delta_4^* = 0.271$. To verify the accuracy of this correlation factor, the first modal damping coefficient for the wet pipe was found experimentally (by filling the pipe with water and plugging it at both ends). An error of approximately 1.1% was found.

The experiments were performed in a closed-circuit water circulation system supplying the pipe with continuous, steady water-flow. This is the same system as that used in previous work (Semler and Païdoussis, 1996; Païdoussis, 1998). It consists of the following components connected by rigid pipes: (i) a water reservoir; (ii) a centrifugal pump; (iii) a variable speed motor; (iv) a water tank used as a pump-pulsation attenuator; (v) an Omega FMG-700 magnetic flow-meter and an Omega DPF60 rate-meter; (vi) a slender flexible pipe; (vii) a collecting tank.

A platform is fitted to the main system, as shown in Fig. 14, acting as a fixed point of attachment for an array of springs giving additional support to the pipe at an intermediate position. A rigid base is clamped onto the main supply pipe of the water-circulation system to which a vertically adjustable platform is attached. The platform slides up and down the rigid base, thus determining the position L_s where the springs are connected to the pipe. The platform is fitted with horizontal sliders to which the fixed ends of the springs are attached, allowing the variation of the initial stretch in each spring, R_o, and their angle θ. The springs are then connected to a thin plastic ring fitted around the pipe at the height of the platform, so that the initial configuration of the array of springs sits in the horizontal plane of the platform.

3.2. Experimental results

3.2.1. First experiment: Case 1 in Table 2

The spring parameters used in the theoretical analysis of Case 1 (see Tables 1 and 2) are the same as those of the first experiment. In this experiment, it proved impossible to eliminate an initial, minute bow in the pipe. Although this bow grew slightly in amplitude as the flow increased, the first important bifurcation was of the Hopf type. The pipe lost stability by planar flutter at a flow rate of $u = 8.8$ in the xy-plane [see Fig. 1(a)], resulting in oscillation about the line of equilibrium. As the flow was further increased, there was a break in the symmetry of the oscillation at $u = 11.7$, i.e., the motion was no longer centred over the line of equilibrium, yet it still remained planar. The system eventually developed unsteady 3-D dynamics.

3.2.2. Second experiment: Case 2 of Table 2

The second experiment corresponds to Case 2 of the theoretical study. A bifurcation diagram obtained experimentally is given in Fig. 15. The physical behaviour of the system depicted therein is as follows. The first instability was static, occurring again in the xy-plane at a flow rate of $u = 6.7$. The amplitude of buckling grew as the flow rate was increased. Eventually, small oscillations developed, superimposed on the divergence state, beginning at a flow velocity of $u = 9.15$. Soon after, while the pipe remained in its state of divergence in the xy-plane, at $u = 10.1$, the pipe lost stability via flutter in the zx-plane, i.e. perpendicular to the initial plane of buckling. This behaviour was labelled "out-of-plane" flutter. The system then returned to in-plane flutter, i.e., in-plane with respect to the original divergence, at $u = 11.54$. The pipe ultimately proceeded to 3-D chaotic oscillations.

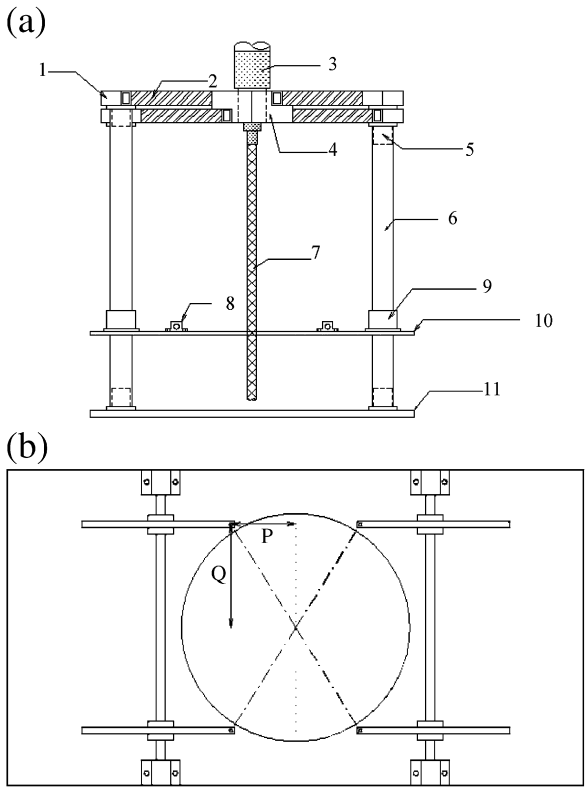

Fig. 14. (a) Side view of the apparatus, showing the base platform that supports the vertically adjustable platform. 1, 2, 4: overlapping z-shaped upper steel supports and central sleeve; 3: supply pipe; 5: boss supporting upper supporting structure; 6: vertical brass pipe post; 7: elastomer pipe; 8: bearing for sliding rod on which one end of the spring is attached; 9: pipe sleeve; 10: vertically adjustable platform; 11: bottom plate with a centred circular hole. (b) Plan-view of the adjustable platform, showing points of attachment of the springs thereon; the pipe is mounted at the centre.

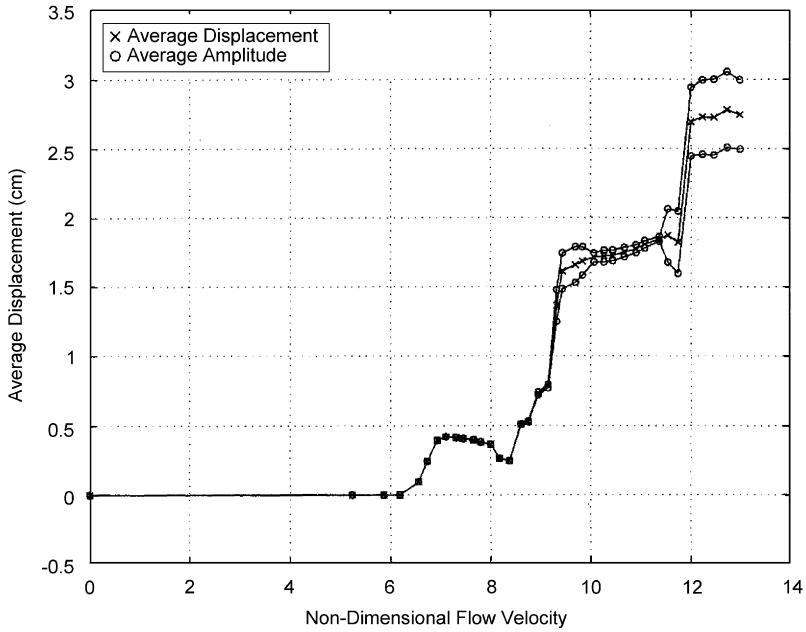

Fig. 15. Experimental bifurcation diagram for Case 2 showing average displacement (×) and average amplitude (○).

3.2.3. Experiments for Cases 4 and 5 of Table 2

While no quantitative data has been recorded for experiments with the parameters for Cases 4 and 5 of Table 2, some interesting, qualitative observations have been made. When attaching two springs to the pipe, such as in Fig. 1(d) with a given angle θ, somewhere between 0° and 45°, and with a slight amount of pre-tension ($R_o > L_o$), the pipe was off its free-hanging centreline in the zx-plane before water even enters the pipe. As the flow rate increased, the pipe remained in its initial, off-centre state. Eventually, the flow rate overcame the structural stiffness of the pipe and caused it to buckle, still in the zx-plane. At even higher flow rate, the pipe lost stability and began to oscillate out-of-plane with the tip displacement tracing a deformed, off-centre figure-of-eight path very similar to that seen in the theoretical results. The Hopf bifurcation here occurred in the xy-plane while the motions in the zx-plane seemed to be uniquely a result of geometrical constraint due to the divergence in that plane.

Similar observations were made for the system with only one spring attached: here the pipe buckled in the plane of the spring and eventually began to flutter predominantly in the perpendicular plane.

These observations report a different behaviour in comparison to the results obtained with the array of four springs, where a Hopf bifurcation occurs in the original plane of divergence before also occurring in the perpendicular plane.

3.2.4. Modified experiments to verify the effect of the ring attachment

As proposed in Part 1, it is thought that moments caused by the ring around the outside of the pipe to which the springs are connected may not be negligible (see Fig. 16). In fact, a simple experiment where the springs are connected in such a way as to eliminate moments in the y-direction, suggests that these moments play an influential role in determining the plane of divergence. The experiment consists in rearranging the spring attachment as shown in Fig. 17. By connecting the springs to the ring of the pipe on the z-axis origin, any possible moment in the y-direction is eliminated. As hoped, the pipe now buckled in the zx-plane, rather than in the xy-plane (as in the experiment with the original method of attachment of the springs); i.e., the pipe buckled in the plane of most resistance. The dynamics then developed in similar fashion as for the experiments for Case 2 where oscillations about the state of divergence emerge, quickly followed by out-of-plane flutter.

4. Comparison of theory and experiments

Comparisons of certain critical flow velocities between experiment and theory are presented in Tables 3 and 4 for Cases 1 and 2, respectively. Unfortunately, most of the quantitative experimental results available for comparison with the theoretical model are confined to the lower flow rates and hence to planar motions.

In the experiment for Case 1, the initial minute divergence is believed to be due to an imperfection in the set-up that could not be eliminated. The first true instability is a Hopf bifurcation, for which the threshold flow velocity is accurately predicted; in fact, the agreement is much better than that usually achieved, i.e., within ~10% (Païdoussis, 1998). It is interesting to see how both experiment and theory predict a break in symmetry about the initial equilibrium at almost the same flow velocity. However, the experimental observations do not record a return to symmetric flutter such as predicted in the numerical results.

For Case 2, the difference between the experimental and theoretical flow rate at which the pipe buckles is larger, but still within 10%. It is important to realize that the flow velocity at which a pipe buckles experimentally is very sensitive to even the slightest imperfection.

The experiments for Case 2 show that the plane of buckling is the xy-plane, while the theoretical model predicts divergence in the zx-plane. As discussed, theory predicts that the pipe buckles in the plane of most resistance. In the experiments, however, the pipe buckled in what theory defines as the plane of least resistance.

In order to explain this paradox, some additional analysis needs to be done. A linear analysis of the system at hand allows the decoupling of the equations of motion in the y- and z-direction. The difference between the two equations lies entirely in the value of the linear spring stiffness terms, κ_{yl} and κ_{zl}:

$$\begin{aligned}
&\eta'''' + \ddot{\eta} + 2u\sqrt{\beta}\dot{\eta}' + u^2\eta'' + \gamma[\eta' - \eta''(1-\xi)] + \kappa_{yl}\eta\delta(\xi-\xi_s) = 0,\\
&\zeta'''' + \ddot{\zeta} + 2u\sqrt{\beta}\dot{\zeta}' + u^2\zeta'' + \gamma\left[\zeta' - \zeta''(1-\xi)\right] + \kappa_{zl}\zeta\delta(\xi-\xi_s) = 0.
\end{aligned} \tag{1}$$

The direction in which the pipe will lose stability first is that for which the predicted u_{cr} is the lowest. Fig. 18 shows how u_{cr} varies as a function of the linear spring stiffness κ (κ_{yl} or κ_{zl}) for $\xi_s = 0.75$, $\beta = 0.145$, and $\gamma = 25.4$. As expected, for low values of κ, a Hopf bifurcation is predicted to occur, and the higher the spring stiffness, the higher is the critical flow velocity. It is also important to notice that u_{cr} changes abruptly in the first portion of the curve. For

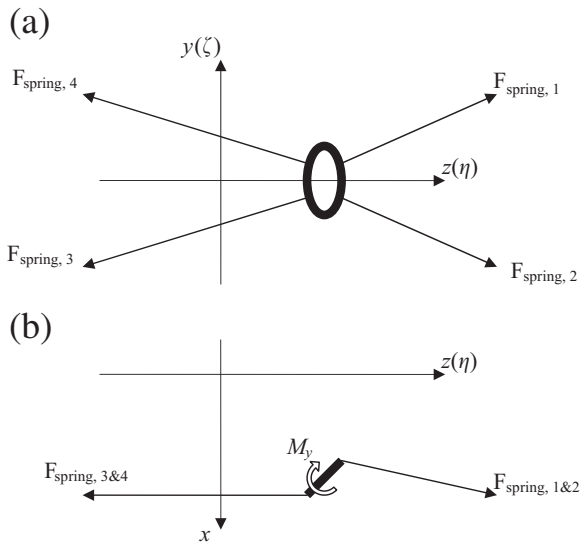

Fig. 16. Representation of the ring fixed to the pipe to which the springs are attached, while the pipe is buckled in the $z(\eta)$-plane. The shown forces come from each individual spring in the array of four springs and create the moment M_y shown in (b). (a) Top view of ring, (b) side view of ring.

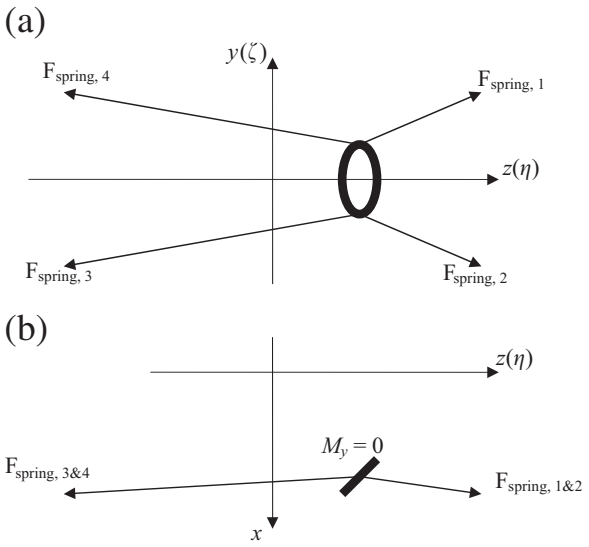

Fig. 17. Representation of the ring onto which the springs are connected to the pipe for the special experiment conducted to verify the effect of the moments acting on the pipe caused by the springs: (a) top view, (b) side view.

stiffness values larger than $\kappa \approx 100$, stability is lost statically through a pitchfork bifurcation and the critical flow velocity decreases asymptotically as the spring stiffness increases.

The linear dimensionless spring coefficients for Case 2 correspond to $\kappa_{yl} = 254.4$ and $\kappa_{zl} = 676.4$. Referring to Fig. 18, for these values of κ the u_{cr} for the pipe in the zx-plane is lower than in the xy-plane, leading to the assertion that the first instability will favour the plane of most resistance (i.e., the zx-plane). Although the values of κ_{yl} and κ_{zl} are significantly different, the respective critical velocities do not differ very much ($u_{cr-y} = 7.50$ versus $u_{cr-z} = 7.47$) due to the asymptotic form in the curve. Since the critical velocities for each plane are so close for the given set of parameters, the plane of divergence can become very sensitive to any kind of imperfection, such as small moments due to the way the springs are connected to the pipe for example.

Table 3
Dimensionless flow velocity, u, for changes in stability of Case 1

	Experimental	Theoretical
Hopf bifurcation	8.8	8.8
Symmetry breaking	11.7	12.2
3-D motion	Not available but observed	15.4

Table 4
Dimensionless flow velocity, u, for changes in stability of Case 2

	Experimental	Theoretical
Static pitchfork bifurcation	6.7	7.3
Hopf about divergence state	9.2	Does not occur
Out-of-plane Hopf; 3-D motion	10.1	8.3

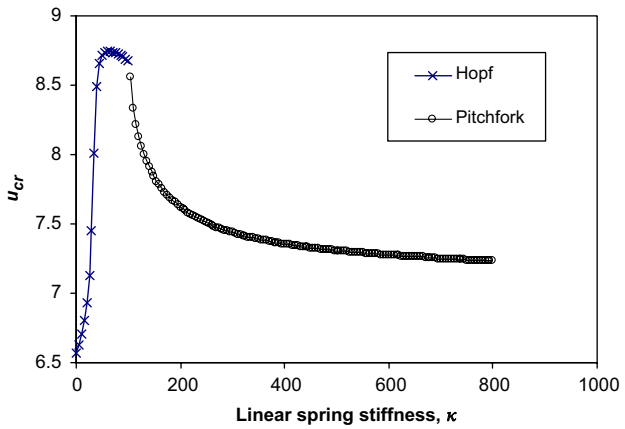

Fig. 18. The critical flow rate, u_{cr}, at which the first bifurcation occurs versus linear spring stiffness, κ. For $\kappa = 0$–100, a bifurcation of the Hopf type occurs; for $\kappa > 100$, pitchfork bifurcations are the first to take place, and u_{cr} follows an asymptotic descent.

Appendix C of Part 1 proposes a linear term that would account for the moments caused by springs that are not connected to the pipe at its centreline. A preliminary linear analysis shows that the moments will increase the flow velocity at which the pitchfork bifurcation occurs in the zx-plane and decrease the same critical velocity in the xy-plane; i.e., the effect is in the right direction. For the actual system parameters, however, the effect is not quantitatively strong enough to switch the plane of divergence (from the plane of least resistance to the plane of most resistance). Only if unrealistic, nonphysical parameters are used (e.g., taking the ring of attachment to be 10 times larger, 10 cm in diameter) does the switching of the plane of divergence take place. At the time of writing, we cannot be certain as to the reason for this important qualitative difference between theory and experiment. It could be that a more accurate 3-D nonlinear modelling of the attachment is necessary, but there may even be some other effect that was not thought of.

5. Conclusion

Utilizing the theoretical model developed in Part 1 of this three-part study (Wadham-Gagnon et al., 2007), here the 3-D nonlinear dynamics of a vertical cantilevered pipe in the presence of additional intraspan spring support has been explored. Choosing parameters corresponding to an experimental system with which comparison is later made, five

particular systems (differing from one another in the location of the spring support, the number of springs involved and their stiffness) have been investigated, referred to as Case 1, Case 2, *et seq*.

In Case 1, the system loses stability via a Hopf bifurcation, leading to planar flutter. With increasing flow, this is followed by a symmetry breaking bifurcation, symmetry reconstitution, and quasiperiodic motions, all planar. The quasiperiodic motions are followed by a radical change in the modal form and frequency of oscillation, from a predominantly travelling-wave form to one characterized by a nodal point near the point of attachment of the springs. At higher flows the oscillation becomes 3-D quasiperiodic, and later chaotic. In the experiments, the initial Hopf and symmetry breaking bifurcations are in excellent agreement with theoretical predictions, as are the modal changes in the oscillations. The onset of quasiperiodic and chaotic motions have also been observed, but some of the finer details of the predicted behaviour have not been observed, and some of the experimental observations are not predicted.

In Case 2, the system loses stability by a pitchfork bifurcation leading to static divergence in the plane where the springs offer most resistance. At higher flow, a secondary bifurcation in that plane and a bifurcation of the trivial solution in the orthogonal plane lead to asymmetric oscillations about the buckled position, initially periodic, and at higher flows quasiperiodic. This is succeeded by periodic figure-of-eight oscillations, and at higher flow by chaotic motion. In the experiments, the qualitative dynamics is generally as predicted, though quantitatively less closely than in Case 1. One aspect where theory and experiment disagree is the plane in which the initial divergence takes place: the plane of most resistance (theory) and the plane of least resistance (experimental). This is investigated in Section 4 and it is found that, for the values of stiffnesses involved in the two directions, the critical flow velocities predicted by the uncoupled linear equations are quite close. It is suspected, therefore, that some detail in the experimental system (not modelled or modelled insufficiently well) is responsible for switching the plane of the initial divergence. In *ad hoc* experiments it was found that when the manner of attachment of the springs to the pipe was modified so as to eliminate the small deformation-induced moment in the usual method of attachment, the plane of divergence switched to that predicted by theory.

In Case 3, instead of a four-spring array as in the foregoing, two co-planar springs were used on either side of the pipe. As the flow velocity is increased, divergence occurs in the plane of the springs, then in-plane flutter is superposed (in the plane of divergence), followed by 3-D figure-of-eight quasiperiodic oscillations. An interesting quasi-intermittent switching is found to occur from in-plane flutter to figure-of-eight oscillations, and an attractive butterfly cross-sectional pattern of motion is observed.

In Cases 4 and 5, the system is initially deformed; two springs as in Fig. 1(d) or a single one draw the pipe off its stretched-straight configuration. As flow is introduced, the system buckles in the plane of most resistance; while in the first case towards the springs, and in the second away from the single spring, the behaviour is globally similar. Then the system develops in-plane flutter in Case 4, followed by 3-D periodic motions; in Case 5, flutter arises simultaneously in the two orthogonal directions, with figure-of-eight periodic motions, followed by chaotic ones.

No experiments are available for comparison with Cases 3–5.

In general terms, it is interesting to remark that, when one Hopf bifurcation occurs in the system, it usually leads to simple periodic oscillations, even when it follows a pitchfork bifurcation. When dynamic bifurcations occur in both planes, theory predicts a much richer dynamical behaviour, ranging from simple periodic cross-sectionally ellipsoidal oscillations and figure-of-eight oscillations to more elaborate 3-D quasiperiodic oscillations.

From these observations, it is quite clear that, at best, the present paper serves to illustrate the very rich dynamical behaviour that this system can develop. Much more remains to be discovered, both by more extensive simulations and a more extensive experimental programme. Specifically, experiments with a different mounting of the springs on the pipe and different location of the springs should be conducted, pipes with different (higher) β should be tested, and corresponding simulations conducted.

Acknowledgements

The authors gratefully acknowledge the support given to this research by the Natural Sciences and Engineering Research Council (NSERC) of Canada. Many thanks also to one of the anonymous referees for some extremely useful comments, leading to significant improvements of this paper.

References

Chen, S.S., 1971a. Flow-induced instability of an elastic tube. ASME Paper No. 71-Vibr-39.
Chen, S.S., 1971b. Dynamic stability of a tube conveying fluid. ASCE Journal of the Engineering Mechanics Division 97, 1469–1485.

Chen, S.S., Jendrzejczyk, J.A., 1985. General characteristics, transition, and control of instability of tubes conveying fluid. Journal of the Acoustical Society of America 77, 887–895.

Edelstein, W.S., Chen, S.S., 1985. Flow-induced instability of an elastic tube with a variable support. Nuclear Engineering and Design 84, 1–11.

Guckenheimer, J., Holmes, P., 1983. Nonlinear Oscillations, Dynamical Systems, and Bifurcation Vector Fields. Springer, New York.

Jendrzejczyk, J.A., Chen, S.S., 1985. Experiments on tubes conveying fluid. Thin-Walled Structures 3, 109–134.

Moon, F.C., 1992. Chaotic and Fractal Dynamics. Wiley, New York.

Païdoussis, M.P., 1998. Fluid–Structure Interactions: Slender Structures and Axial Flow. Academic Press, London.

Païdoussis, M.P., Semler, C., 1993. Nonlinear dynamics of a fluid-conveying cantilevered pipe with an intermediate spring support. Journal of Fluids and Structures 7, 269–298.

Païdoussis, M.P., Semler, C., 1998. Non-linear dynamics of a fluid-conveying cantilevered pipe with a small mass attached at the free end. Journal of Non-Linear Mechanics 33, 15–32.

Saaid, S., 1999. Nonlinear dynamics of a fluid-conveying cantilevered pipe with an intermediate nonlinear spring support. B.Eng. Honours Thesis, Department of Mechanical Engineering, McGill University, Montreal, Québec, Canada.

Semler, C., Païdoussis, M.P., 1996. Nonlinear analysis of the parametric resonances of a planar fluid-conveying cantilevered pipe. Journal of Fluids and Structures 10, 787–825.

Steindl, A., 1996. Heteroclinic cycles in the dynamics of a fluid conveying tube. In: Kirchgassner, K., Mahrenzoltz, O., Mennicken, R. (Eds.), Proceedings of the ICIAM Conference. Akademie-Verlag, Berlin, pp. 529–532.

Steindl, A., Troger, H., 1996. Heteroclinic cycles in the three-dimensional postbifurcation motion of O(2)-symmetric fluid conveying tubes. Applied Mathematics and Computation 78, 269–277.

Sugiyama, Y., Tanaka, Y., Kishi, T., Kawagoe, H., 1985. Effect of a spring support on the stability of pipes conveying fluid. Journal of Sound and Vibration 100, 257–270.

Wadham-Gagnon, M., Païdoussis, M.P., Semler, C., 2007. Dynamics of cantilevered pipes conveying fluid. Part 1: nonlinear equations of three-dimensional motion. Journal of Fluids and Structures 23, doi:10.1016/j.jfluidstructs.2006.10.009.